www.rericjournal.ait.ac.th

Yearly Energetic and Exergetic Performance of Solar Absorption Refrigeration System in the Region of Northern Sudan

Osman Wageiallah Mohammed* and Guo Yanling*,[1]

Abstract – *Utilizing solar energy to drive cooling systems is an attractive idea since the need for cooling is nearly in phase with solar energy availability. It is particularly true in the region of Northern Sudan where solar resources are among the highest in the world. In this study, the cooling production, energetic performance (COP) and exergy efficiency (EE) of a solar-driven absorption refrigeration system in Northern Sudan have been investigated. The proposed system is a 100 kW (cooling capacity) NH_3/H_2O absorption system driven by high efficiency flat-plate solar collectors instead of the evacuated tube collectors in vogue which are much expensive. The results showed that the system yields maximum power during May and it is minimum in December. The system can produce 591.2 kWh in 8 hours during May with daily average COP and EE equal to 0.4481 and 0.2999, respectively. While production is declined to 490 kWh in 7 hours per day with average COP and EE values of 0.446 and 0.3335 in December. These results demonstrated that the NH_3/H_2O absorption refrigeration systems can be driven by flat-plate collectors in Northern Sudan, throughout the year, with relatively good performance. This can effectively decrease the system's initial cost here and at other places to that possess similar solar resources.*

Keywords – absorption refrigeration cycle (ARC), energy analysis, exergy analysis, Northern Sudan, solar energy.

[1] 1. INTRODUCTION

During last century, fossil fuels have been considered as the main source of energy [1], [2]. However, its non-renewable origin and negative impacts on the environment have seriously necessitated the need of research for usage of renewable energy sources [3], [4]. Among all renewable and environment friendly sources, solar energy has a characteristic distinction due to its large availability and enormous potential [5]. Further, along the globe many rural areas have abundant solar energy supplies, nevertheless suffer from shortage of electricity. Therefore, the idea of using available solar energy to drive a cooling system for cold storage seems to be an attractive idea. It will be quite beneficial especially in developing countries where problem of food preservation is often as painstaking as food production [6]. For solar-driven refrigeration systems the ammonia-water (NH_3/H_2O) absorption cycle has been regarded as one of the best options since it can freeze water and hence can store the cold. However, high initial costs of such systems have remained a stumbling block to their widespread.

The region of Northern Sudan consists of two states, River Nile State (Nahr an Nil) and Northern State (Ash-Shamaliyah). Area of this region is about 471×10^3 km^2 which represents about 25% of the total area of the Sudan. The climate here is of typical desert type according to Köppen climate classification [7]. Summer is very hot, mean maximum temperature reaches 43.4°C, annual average of relative humidity is only about 25%, sunshine is very prevalent and the rains are rare [8]. This region has ample solar energy resources. Average annual solar radiation intensity reaches 8200-8700 MJ/m^2 which corresponds to 2300-2400 kW/m^2 (6.3-6.63kW/m^2.day) [8]. Annual average sunshine hours range between 3650 to 3830 hours. These values for solar resources are among the highest in the world [9], [10]. Main activity of population in the region is cultivation of vegetables, fruits, and grains on the banks of the Nile River. Cooling is essential for both refrigeration and air conditioning in this blistering region to increase the shelf life and keeping quality of fruits, vegetables, and other perishable products. For this purpose, a solar-driven single-stage NH_3/H_2O absorption refrigeration system is proposed to supply a cold storage in the study area. Flat plate solar collectors (FPC) are the most used type of solar collectors. In this region with huge solar resources such collectors can play an important role. Their advantages are: relatively inexpensive, can utilize both of beam and diffuse solar radiation, require little maintenance and no need for tracking system [11]. Well-designed FPC can deliver energy at temperatures as high as 100°C above ambient [12]. Recent innovation of highly selective coatings like TiNOX has made it easy to reach more than 200°C stagnation temperatures [13], [14]. So, in present study a high performance FPC is suggested to drive the proposed ARS in Northern Sudan.

Performance of a solar cooling system is strongly dependent on local conditions. Solar cooling systems can be efficiently operated in locations where sufficient solar radiation and good heat sink are available [15], [16]. Therefore, prior to the designing of these systems, it is indispensable to undertake appropriate investigation regarding the performance and expected output according to local conditions. For evaluation of system's efficiency, the coefficient of performance (COP) and exergy efficiency (EE) are usually used [17], [18]. First parameter (COP) is the ratio of useful energy gained by

*College of Mechanical and Electrical Engineering, Northeast Forestry University, Harbin 15000, PR China.

[1]Corresponding author;
Tel: +86 1391891026.
Email: guo.yl@hotmail.com.

the evaporator to the heat energy supplied to the generator and mechanical power consumed by the pump. Second parameter (EE) shows how effectively the system employs given energy resources [19], [20]. For absorption refrigeration system it is defined as the ratio of exergy gained by evaporator to exergy flow to generator and pump [21], [18].

By surveying the literature in the field of continuous solar refrigeration some studies have been found. Sozen *et al.* [22] performed an experimental study for the system under climate of Ankara, Turkey. The system was driven by a parabolic collector. Their results showed that exergy loss in absorber and evaporator is higher than other system components. Aman *et al.* [17] executed a simulation analysis of a 10 kW single-effect NH_3/H_2O solar absorption system for air-conditioning. At generator, condenser/ absorber and evaporator temperatures of 80°C, 30°C and 2°C, respectively, the achieved values of COP and EE are 0.60 and 0.3201. The study also uncovered that 63% of total exergy loss occurs in the absorber. Recently, Said *et al.* [3] empirically studied a similar system under climate of Saudi Arabia. The system was 10 kW cooling capacity driven by a set of evacuated collectors (CPC-18). The results indicated maximum value of COP at generator/condenser/ evaporator temperatures of 114/23/-2 (°C).

For exploration of the system's performance under Sudan climate, only two studies could be reviewed. In 1988, Soletjes *et al.* [23], experimentally studied a 13 kW peak cooling power ammonia-water (NH_3/H_2O) absorption refrigeration system driven by evacuated solar collectors. The system was designed to keep 10 tons of agricultural products at 5°C in a cold store. The system was tested at Soba (central Sudan) and it performed well. Major impediment as reported by the authors was the high initial cost of the system, mainly due to the usage of expensive solar collectors. Lately, Manahil designed, constructed and tested a prototype of NH_3/H_2O solar absorption refrigeration system with 0.111 kW cooling power. The system was operated by evacuated tube solar collectors and was used as a laboratory test device to evaluate the performance of system's components [24].

In all mentioned studies, the high system's performance was achieved by utilizing either parabolic or evacuated-tube solar collectors. These types of solar collectors can give good output even in places which have low density solar radiation [12]. However, their relatively high prices increase the system's initial cost to a great extent. As reported by some authors, in solar absorption cooling systems which utilize concentrated and evacuated solar collectors, cost of collector's array alone can be more than 50% of the whole system's cost [25]. The main objective of this study is to explore the performance of an optimized NH_3/H_2O solar absorption refrigeration system under the climate of Northern Sudan. To reduce the initial cost, suggested system is driven by high performance FPC, so that the potential of this collector type to drive absorption system in study area will be quantified.

2. SYSTEM DESCRIPTION

The system is a single stage NH_3/H_2O absorption refrigeration system driven by hot water from high-efficiency FPC. Major components are: solar collectors' field, generator, rectifier, water-cooled condenser, evaporator, water-cooled absorber and two heat exchangers; solution heat exchanger (SHX) and refrigerant heat exchanger (RHX). The system's configuration is shown in Figure 1.

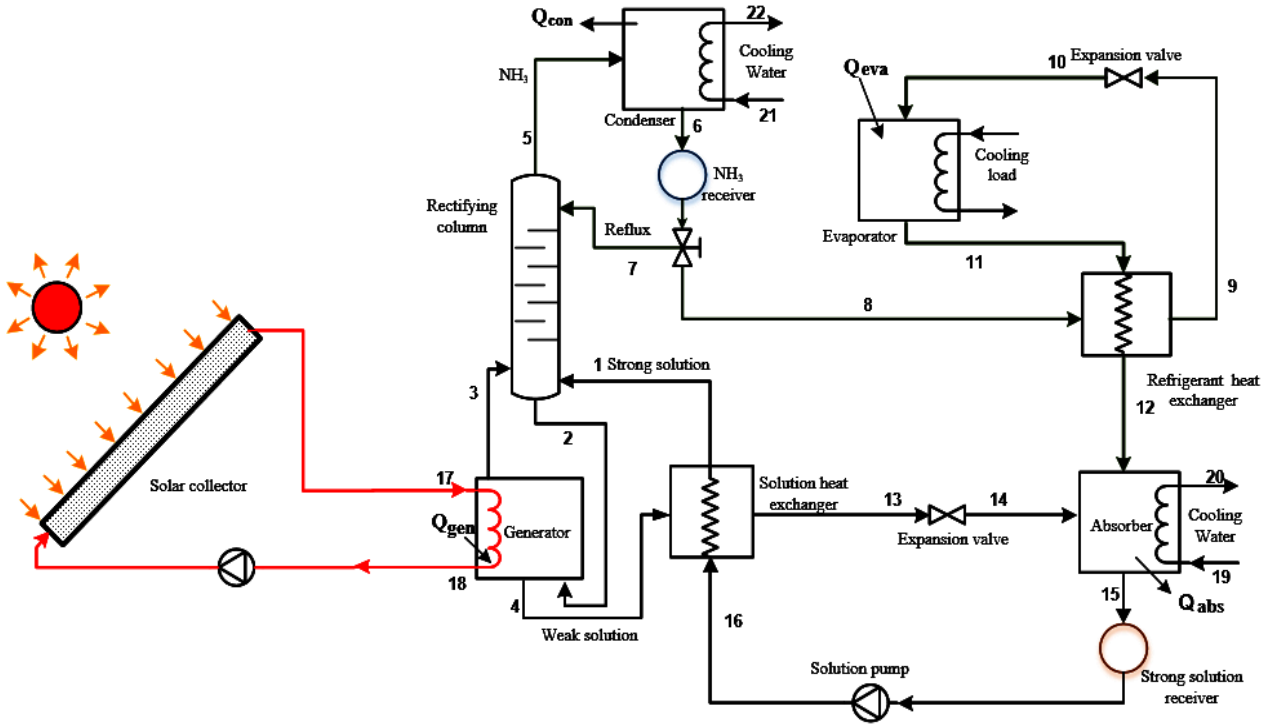

Fig. 1. Ammonia-water solar absorption refrigeration system.

Hot water from solar collector field is fed directly to the generator for heating strong solution and generate ammonia vapor at high pressure. At the same time some water vapor is generated and passes with ammonia vapor to the rectifier where they are separated. Only ammonia vapor with high concentration (0.998) is sent to the condenser to form refrigerant and later collected in ammonia receiver. Small fraction of the refrigerant returns to the rectifier as a reflux. Remaining refrigerant passes through the RHX where it is sub-cooled by evaporated refrigerant that leaving the evaporator and before entering the absorber. Then, the sub-cooled refrigerant passes through expansion valve to get evaporated in the evaporator at low temperature to induce cooling effect. After evaporator it passes through RHX to reach the absorber where it is absorbed by weak solution (returning from the generator) to form strong solution. At this step, strong solution is sent by solution pump through the SHX where it is preheated by the weak solution, before it reaches the generator.

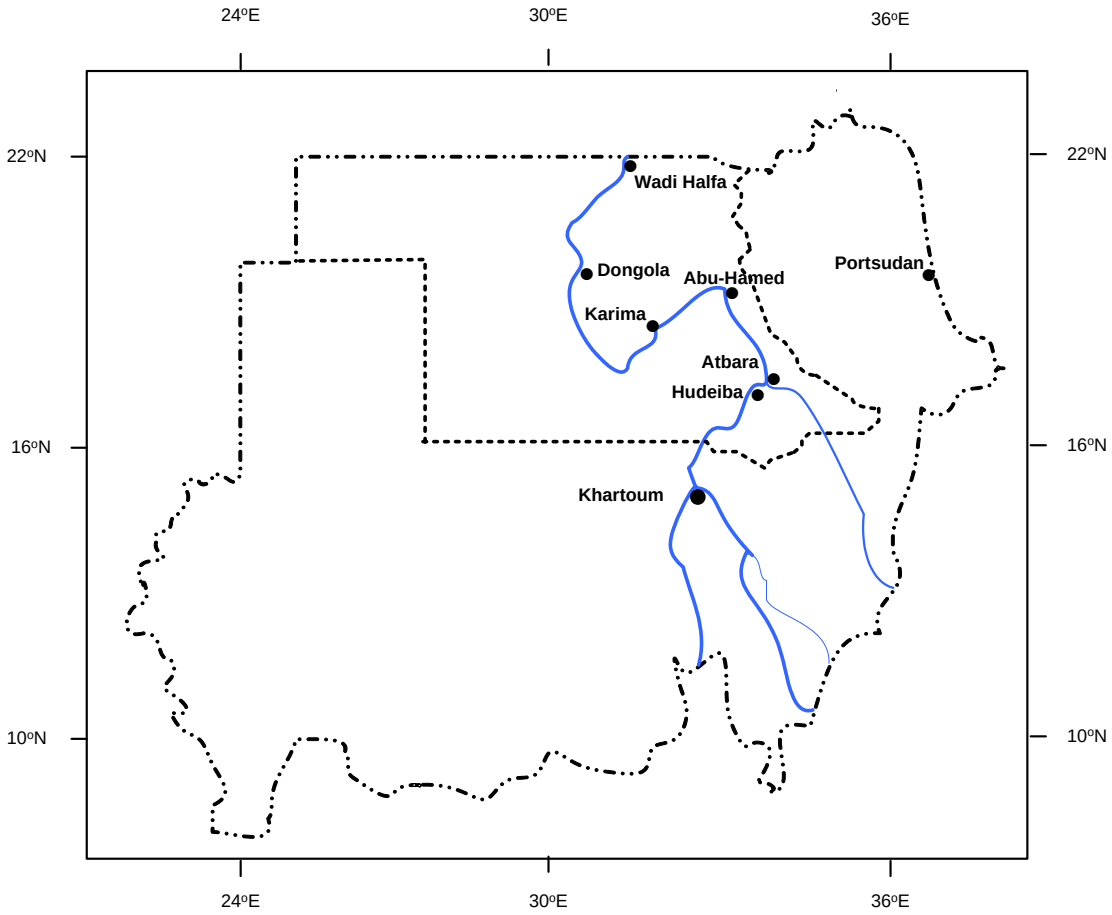

Fig. 2. Region of Northern Sudan and stations under consideration.

3. SOLAR ENERGY IN NORTHERN SUDAN

Amount of available solar energy in a particular place must be known to solar engineers and designers prior to embark upon any such study. Figure 2 shows the area covered by this study. It extends between longitudes 25^{o} 3` E to $35^{o}$ 30` E and latitudes 16^{o} N to 22^{o} N. In this vast tract there are two meteorological stations having records for measurements of monthly average global solar radiation (Hudeiba and Dongola stations). Sunshine duration, however, is measured at six stations (Hudeiba, Atbara, Abu-Hamed, Karima, Dongola, and Wadi-Halfa). Therefore, for stations lacking measurements of global solar radiation, the used data is taken from [6]. Values of the monthly average sunshine duration and global solar radiation at six stations in study area are depicted in Figures 3 and 4, respectively.

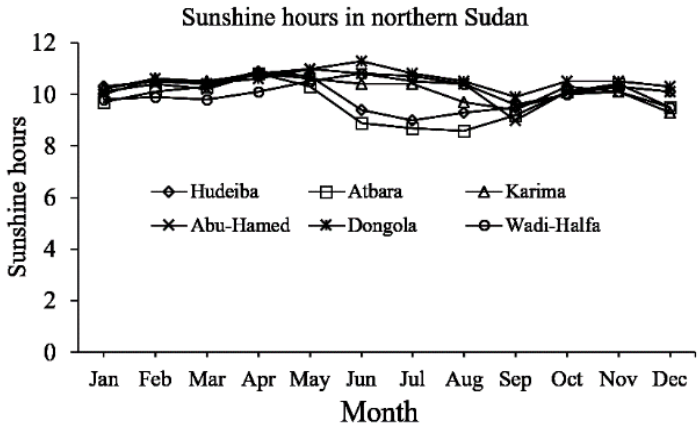

Fig. 3. Sunshine duration in region of Northern Sudan [6].

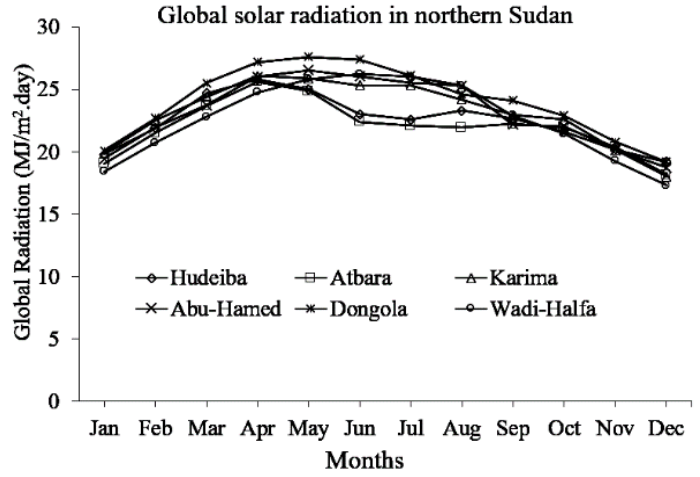

Fig. 4. Global solar radiation in region of Northern Sudan [6].

4. SYSTEM MODELING

The solar absorption refrigeration system shown in Figure 1 can be divided into two subsystems: cooling sub-system and solar sub-system. Former part consists of absorption cycle and the later comprise of solar collectors and pump.

4.1 Modeling of the Absorption System

Analysis of the absorption system was carried out on the basis of following assumptions:

- The strong solution at the absorber outlet is saturated at the absorber temperature.
- The refrigerant at the condenser outlet is saturated at the condenser temperature.
- The weak solution leaves generator at its temperature.
- The rectifier has a constant efficiency.
- The vapor at the rectifier outlet is saturated at its pressure and mass concentration.
- Complete condensation takes place through the condenser.
- The refrigerant passing through condenser, evaporator and RHX is not pure ammonia (ammonia concentration in refrigerant is 0.998), so the effects of water presence in refrigerant are considered in this study.

Values of some parameters were taken at their practical values from previous studies. So at the base condition: effectiveness of the SHX and RHX were 0.8 and 0.7, respectively. Pump efficiency was taken as 0.65, refrigerant concentration as 0.998 and reflux ratio as 0.2 [26]. Temperature of the heating water was assumed to be decreased by 10°C as it passes through the generator. The pressure losses were taken as ΔP/P = 0.05 between the generator and condenser while ΔP/P = 0.075 between the evaporator and absorber. Here P is the pressure at the pipe exit [27]. Simulation model was developed to evaluate the performance of a single-stage NH_3/H_2O ARS. The developed model is based on energy, mass and species conservation equations. General forms of these equations are specified as follows:

Energy conservation:

$$\sum(\dot{m}h)_{in} - \sum(\dot{m}h)_{out} + \left[\sum \dot{Q}_{in} - \sum \dot{Q}_{out}\right] \pm W = 0 \quad (1)$$

Mass conservation:

$$\sum \dot{m}_{in} - \sum \dot{m}_{out} = 0 \quad (2)$$

Exergy balance-

$$\sum \dot{E}_{in} - \sum \dot{E}_{out} + \sum \left(1 - \frac{T_o}{T_j}\right) \dot{Q}_j = \sum \dot{E}_{dest} \quad (3)$$

In ammonia water systems, the solution concentration varies during the system processes which changes the chemical exergy of the working fluid [28]. Therefore, in Equation 3 $\dot{E}$ constitutes the thermo-mechanical and a chemical exergy. By applying these general forms to each individual component in the system, energy, mass and exergy balances can be written as summarized in Table 1.

The performance of absorption refrigeration systems (ARSs) is usually measured by the coefficient of performance (COP), exergy efficiency (EE) and circulation ratio (CR). The COP for absorption refrigeration system is given by:

$$COP = \frac{\dot{Q}_{eva}}{\dot{Q}_{gen} + \dot{W}_{pump}} \quad (4)$$

The EE is given by [17], [18] as:

$$EE = \frac{|\dot{E}_{eva}|}{\dot{E}_{gen} + \dot{E}_{pump}} = -\frac{\dot{Q}_{eva}(1 - T_o/T_{eva})}{\dot{Q}_{gen}(1 - T_o/T_{gen}) + \dot{W}_{pump}} \quad (5)$$

Where $\dot{E}$ is the exergy transfer rate (W). The reference temperature (T_o) is taken as 25°C [29]. Circulation ratio for the system is derived by:

$$CR = \frac{\dot{m}_{ss}}{\dot{m}_r} \quad (6)$$

In order to compute all energy and mass balances used in the thermodynamic analysis of the considered absorption system, the simulation software *Cycle-Tempo* is used. This program allows the user to assemble the components of the system graphically, input the necessary data and solve the system of equations formed by mass and energy balances simultaneously with a robust algorithm [30]. The thermodynamic properties of NH_3/H_2O mixture were obtained by equations of Ziegler and Trepp [31] implemented in the software.

Table 1. Mass, energy and exergy relations for each component of the system.

Component	Mass balance	Energy balance	Exergy balance
Generator	$\dot{m}_2 = \dot{m}_3 + \dot{m}_4$	$\dot{Q}_{gen} = \dot{m}_3 h_3 + \dot{m}_4 h_4 - \dot{m}_2 h_2$	$\dot{E}_{dest,gen} = \dot{m}_2 E_2 - \dot{m}_3 E_3 - \dot{m}_4 E_4 + \dot{Q}_{gen}[1 - (T_o/T_{gen})]$
Rectifier	$\dot{m}_2 + \dot{m}_5 = \dot{m}_1 + \dot{m}_3 + \dot{m}_7$	$\dot{m}_2 h_2 + \dot{m}_5 h_5 = \dot{m}_1 h_1 + \dot{m}_3 h_3 + \dot{m}_7 h_7$	$\dot{E}_{dest,rect} = \dot{m}_1 E_1 + \dot{m}_3 E_3 + \dot{m}_7 E_7 - \dot{m}_2 E_2 - \dot{m}_5 E_5$
Condenser	$\dot{m}_5 = \dot{m}_6$	$\dot{Q}_{cond} = \dot{m}_5 h_5 - \dot{m}_6 h_6$	$\dot{E}_{dest,cond} = \dot{m}_5(E_5 - E_6) - \dot{Q}_{cond}[1 - (T_o/T_{cond})]$
RHX	$\dot{m}_8 = \dot{m}_9, \dot{m}_{11} = \dot{m}_{12}$	$\dot{Q}_{RHX} = \dot{m}_8(h_8 - h_9) = \dot{m}_r(h_{12} - h_{11})$	$\dot{E}_{dest,RHX} = \dot{m}_8(E_8 - E_9 + E_{11} - E_{12})$
Evaporator	$\dot{m}_{10} = \dot{m}_{11}$	$\dot{Q}_{eva} = \dot{m}_8(h_{11} - h_{10})$	$\dot{E}_{dest,eva} = \dot{m}_8(E_{10} - E_{11}) + \dot{Q}_{eva}[1 - (T_o/T_{eva})]$
Absorber	$\dot{m}_{12} + \dot{m}_{14} = \dot{m}_{15}$	$\dot{Q}_{abs} = \dot{m}_{12} h_{12} + \dot{m}_{14} h_{14} - \dot{m}_{15} h_{15}$	$\dot{E}_{dest,abs} = \dot{m}_{12} E_{12} + \dot{m}_{14} E_{14} - \dot{m}_{15} E_{15} - \dot{Q}_{abs}[1 - (T_o/T_{abs})]$
Pump	$\dot{m}_{15} = \dot{m}_{16}$	$\dot{m}_{15} h_{15} + \dot{W}_{pump} = \dot{m}_{16} h_{16}$	$\dot{E}_{dest,pump} = \dot{m}_{15}(E_{15} - E_{16}) + \dot{W}_{pump}$
SHX	$\dot{m}_4 = \dot{m}_{13}, \dot{m}_{16} = \dot{m}_1$	$\dot{Q}_{SHX} = \dot{m}_4(h_4 - h_{13}) = \dot{m}_{16}(h_1 - h_{16})$	$\dot{E}_{dest,SHX} = \dot{m}_4(E_4 - E_{13}) + \dot{m}_{16}(E_{16} - E_1)$
RV	$\dot{m}_9 = \dot{m}_{10}$	$h_9 = h_{10}$	$\dot{E}_{dest,RV} = \dot{m}_9(E_9 - E_{10})$
SV	$\dot{m}_{13} = \dot{m}_{14}$	$h_{13} = h_{14}$	$\dot{E}_{dest,SV} = \frac{\dot{m}_{13}(P_{13} - P_{14})}{P_{13}}$

4.2 Modeling of the Solar Collector

In solar absorption refrigeration systems driven by flat-plate collectors, performance of the collector is of primary concern. Reason being those systems require relatively high driving temperatures with respect to the range of temperatures that can be reached by ordinary FPC. So a high efficiency flat-plate solar collector has been considered in this study. To achieve high absorptance (α) and low emittance (ε) for collector's plate selective coating material TiNOX is used (α = 0.95, ε = 0.05) [13], [14]. Specifications of the used collector are tabulated in Table 1. Analysis of the collector was performed on the basis of following assumptions:

- The collector operates in steady state.
- Uniform flow inside the tubes.

- The headers cover a small area of collector and can be neglected.
- The sky can be considered as a black body for long-wavelength at an equivalent sky temperature. The area of absorber is assumed to be same as the frontal transparent area.
- Properties are independent of temperature.
- There is one-dimensional heat flow through the back and side insulation and through the cover.

Instantaneous efficiency of FPC is arrived by:

$$\eta = \frac{Q_u}{A_c G_T} = F_R(\tau\alpha) - F_R U_L \frac{(T_i - T_a)}{G_T} \quad (7)$$

Where, Q_u is the useful energy gain by collector (W), A_c is the collector gross area (m^2), G_T is the intensity of incident solar radiation (Wm^{-2}), F_R is collector heat removal factor, ($\tau\alpha$) the transmittance-absorptance product of cover-plate system is calculated in *CoDePro* program by Equation 9 , U_L is the overall heat loss coefficient ($Wm^{-2}K^{-1}$), T_i is the inlet fluid temperature (^oC) and T_a is the ambient temperature (^oC) [32]. The collector useful gain Q_u is given as:

$$Q_u = [A_p S - A_c U_L (T_{pm} - T_a)] \quad (8)$$

Here A_p is the collector aperture area (m^2), T_{pm} is the mean absorber plate temperature (^oC). S is the absorbed solar radiation per unit area of collector's absorber (Wm^{-2}). Transmittance-absorptance product ($\tau\alpha$) is given by [12]:

$$(\tau\alpha) = \tau\alpha \sum_{n=0}^{\infty} [(1-\alpha)\rho_d]^n = \frac{\tau\alpha}{1-(1-\alpha)\rho_d} \quad (9)$$

Where, ρ_d is the cover system reflectance for diffuse radiation coming from bottom side.

The collector heat removal factor F_R is attained by:

$$F_R = \frac{\dot{m} C_p (T_o - T_i)}{A_c [S - U_L^{'}(T_i - T_a)]} \quad (10)$$

Here $U_L^{'}$ is the overall loss coefficient based on aperture area and $\dot{m}c_p$ is the heat capacity of collector fluid ($W\ K^{-1}$).

According to ASHRAE standard, instantaneous efficiency can also be expressed as:

$$\eta = a_0 + a_1 \frac{\Delta T}{G_T} + a_2 \left(\frac{\Delta T}{G_T}\right)^2 \quad (11)$$

Where $\Delta T = T_i - T_a$.

In this study flat-plate collector design program (*CoDePro*) was used for designing, optimization and output investigation of the solar collector [32]. For this purpose, specifications in Table 2 with data of weather (temperature, humidity and wind speed) and solar radiation for the specific locations were employed. The program calculates all required values which include ($\tau\alpha$), U_L (contains top, bottom, and edges losses), F_R, Q_u and the temperature of water at collector outlet (T_o) along with the collector efficiency (η_i).

4.3 Model Validation

The absorption system model has been validated by applying the set of data taken from [26]. The comparison between several key values computed by the model and those published in the cited reference is presented in Tables 3a and 3b. As shown, the results of the model are close to that in mentioned reference. Likewise, validation of flat plate solar collector has been conducted. For this purpose the calculated results for collector's instantaneous efficiency have been compared with experimental values reported in [32]. Efficiency of MSC-32 flat plate collector are plotted as a function of $\Delta T/G_T$, along with the predicted values in Figure 5.

As revealed by this figure, calculated results by *CoDePro* are in a close agreement with the experimental results.

Table 2. Collector material and dimensions.

Components	Specifications	Components	Specifications
Collector gross surface	3.64 m^2	Absorber Emittance (ε)	0.05
Absorber surface	3.373 m^2	Tube Material	copper
Frame	Aluminium Alloy 0.05 m	Tube inner Diameter	10 mm
Length × width × thickness	2.8 × 1.3 × 0.184 m	Tube thickness	1 mm
Glazing	Single Cover, 3.2 mm glass Transmittance 0.891	Number of tubes	13
Bottom Insulation	0.05 m urethane	Tube-To tube Spacing	95.4 mm
Edge Insulation	0.04 m urethane	Collector Flow Rate	0.02 l/s (kg/s)
Absorber Material	Copper 3 mm thickness	Collector Capacity	0.004 m^3
Absorber coating	TiNOX	Plate-tube bond Conductance	400 W/m K
Absorber Absorptance (α)	0.95	Header Tube diameter	25mm

Table 3a. Absorption model validation, temperature, pressure and flowrates.

Stream No.	Temperature (°C)		Pressure (bar)		Mass flow (kg/s)	
	Ref.[26]	model	Ref.[26]	model	Ref.[26]	model
1	90.4	90.4	17.28	17.28	38.761	38.758
4	120.0	120.0	17.28	17.28	30.449	30.447
5	63.6	63.6	17.28	17.28	9.553	9.552
6	44.0	44.0	17.28	17.28	9.553	9.553
9	-5.14	-5.14	17.28	17.28	8.311	8.311
10	-10.6	-10.6	2.83	2.83	8.311	8.311
11	-10.0	-10.0	2.83	2.83	8.311	8.311
12	24.0	24.0	2.83	2.83	8.311	8.311
13	36.8	36.8	17.28	17.28	30.449	30.447
14	37.1	37.1	2.83	2.83	30.449	30.447
15	25.0	25.0	2.71	2.71	38.761	38.758
16	25.3	25.3	17.28	17.28	38.761	38.758
17	44.0	44.0	17.28	17.28	1.242	1.242

Table 3b. Absorption model validation, energy flow and COP.

Thermal Loads (kW) and COP		
quantity	Ref.[26]	model
$\dot{Q}_{eva}$	9574.34	9574.34
$\dot{Q}_{gen}$	16197.1	16197.4
$\dot{Q}_{con}$	10971.8	10971.8
$\dot{Q}_{abs}$	14691.2	14692.4
$\dot{Q}_{SHX}$	11651.1	11651.0
$\dot{Q}_{RHX}$	1941.23	1941.22

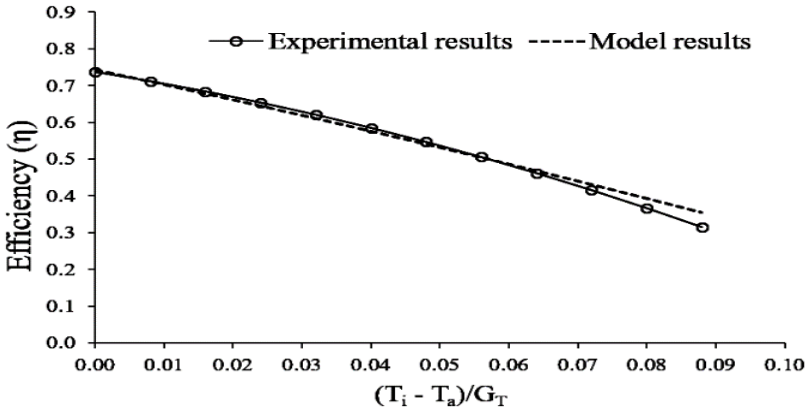

Fig. 5. Comparison between measured and predicted collector efficiency.

5. RESULTS AND DISCUSSION

In the region of Northern Sudan as illustrated by Figure 4, during a year, monthly average daily global solar radiation reaches its maximum value (27.60 MJ/m^{2}day) in the month of May at Dongola. It touches the minimum value (17.31 MJ/m^2.day) in December at Wadi-Halfa. These two values represent the expected range of available solar energy in this region. Therefore, the performance of system under consideration has been examined by using Dongola data in the month of May and Wadi-Halfa data during the month of December to represent the maximum and minimum of the expected output along the region. Results are discussed in following sections.

5.1 Effect of Operating Parameters on Absorption System Performance

In order to make appropriate choice for values of generator condenser and evaporator temperatures, their effects on system performance have been studied. The results are displayed graphically by varying the

parameter under consideration while keeping other parameters at their base values.

5.1.1 Effect of Generator Temperature

The generator temperature (T_{gen}) is one of the most important parameters affecting the performance of absorption systems. The COP and EE of system were plotted as functions of T_{gen} in Figure 6. The T_{gen} varied from cut-in/off limit to 120°C while keeping all other parameters constant at their base values.

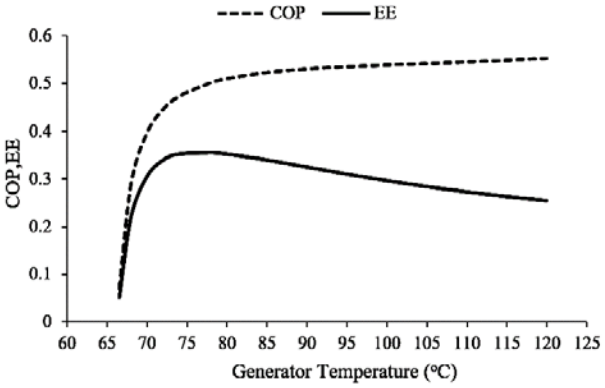

Fig. 6. Effect of generator temperature in COP and EE.

As T_{gen} increases the COP rapidly increases until about 90°C, after that gradient of the COP curve becomes nearly flat. Meanwhile, the EE pass through maxima at 76°C and decreases gradually on ward. This suggests that the exergetic performance of the system is more sensitive to high T_{gen} than the energetic performance. This behavior can be attributed to increase in the solution temperature in the generator and absorber which leads to more exergy losses in two components [27], [22]. These results are in a good agreement with those reported in [17], [33].

5.1.2 Effect of Condenser Temperature

Figure 7 revealed the relationships between COP, EE and condenser temperature. Here T_{con} varies from 20 to 42°C which corresponds to the change in condensation pressure from 8.557 to 16.42 bar. The COP is decreased from 0.5418 to 0.3311 and the EE is decreased from 0.3338 to 0.1846 which endorse the findings published by Aman *et al.* [17]. These results can be explained as follows: for constant Q_{eva}, increasing the T_{con} means a higher pressure in the generator, so more heat is required (higher Q_{gen}) to produce ammonia vapor. Consequently higher exergy loss occurs in generator.

5.1.3 Effect of Evaporator Temperature

Effect of the evaporator temperature (T_{eva}) on system's performance is illustrated in Figure 8. The T_{eva} varies from -12 to 12°C which raises the COP from 0.4838 to 0.5633. Higher T_{eva} increases absorber pressure which rise ammonia concentration in outgoing solution. This decreases Q_{gen} and leading COP to increase. On the contrary, as the T_{eva} increases EE declines sharply from 0.3691 to 0.1422, so increasing T_{eva} has a negative effect on EE. This result is expected because the evaporator has a higher potential for cooling at a lower temperature which agrees with the results reported in [17].

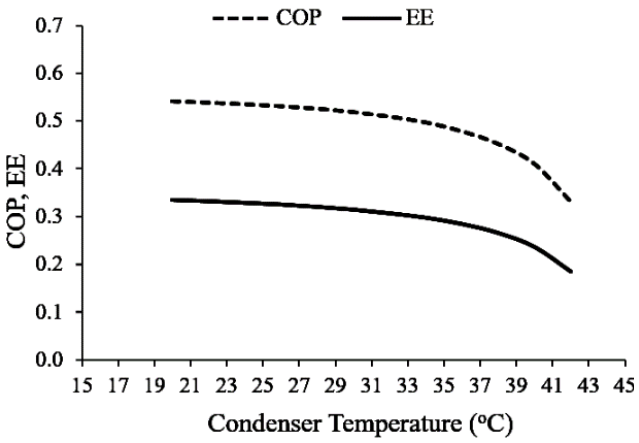

Fig. 7. Effect of condenser temperature in COP and EE.

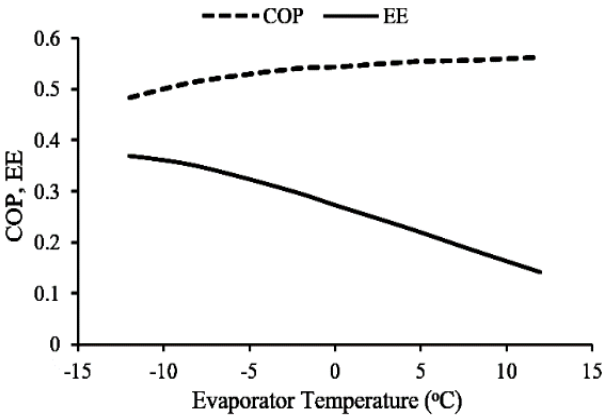

Fig. 8. Effect of evaporator temperature in COP and EE.

5.2 The Collector Output

By using solar radiation data presented in Figures 3 and 4, appropriate equations from [12], specifications in Table 1 and weather data for Dongola and Wadi-Halfa as inputs in *CoDePro*, the useful energy gain and collector performance have been obtained. Time in all stated results is the solar time. For maximum energy availability, the collector was oriented southwards with a slope of 15° less than the latitude in summer and 15° more than the latitude in winter [12].

As shown by Figure 9, solar collector yields its maximum output during the month of May (in Dongola). It occurs at solar noon i.e. for the hour 11:30 AM to 12:30 PM when the sun is nearly vertical to the collector. At that time the incident solar radiation on tilted collector is about 1020 W/m^2, ambient temperature and air speed are 42°C and 4.5 m/s, respectively. So the collector is working in typical conditions. Also during this hour the collector reaches its highest efficiency (61.8%) as displayed by Figure 10 and the hot water at the collector outlet reaches its maximum temperature (96°C) as illustrated by Figure 11.

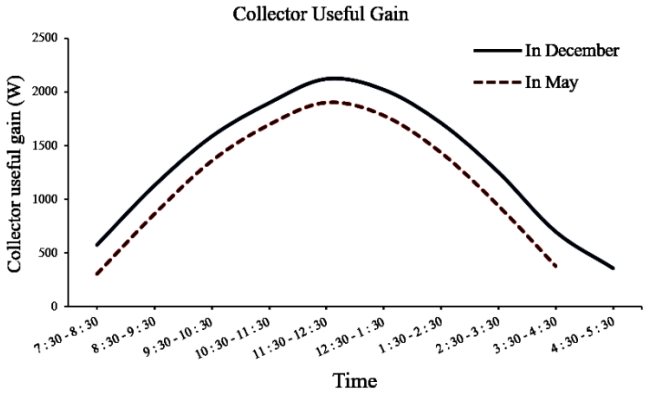

Fig. 9. The solar collector useful energy gain in Northern Sudan.

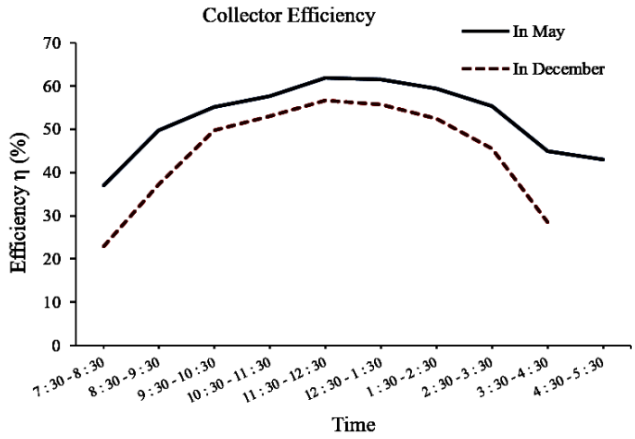

Fig. 10. The solar collector efficiency in Northern Sudan.

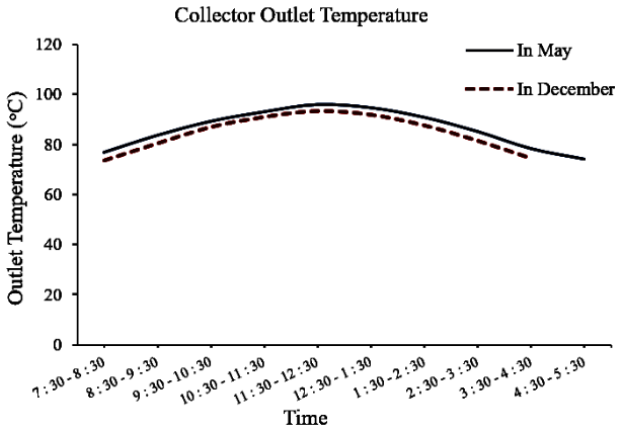

Fig. 11. Collector outlet temperature in Northern Sudan.

During the month of May the collector have a useful energy gain for 10 hours, the hot water temperature is above 90°C for 4 hours and is above 80°C for 7 hours per day. Before 7:30 AM the useful energy is very low, hence the collector pump must be turned off so that the incident energy can heat the collector and its fittings. Accordingly after 5:30 PM the collector pump must be turned off since the useful gain is very low. The energy gain per day during the month of May, by 1 m^2 of the collector absorber area, is 14.45 MJ/m^2.day which is equal to 4.02 kWh. As it is expected, during the month of December (in Wadi-Halfa) output of the collector is relatively lower than that in the month of May. Maximum values of hot water temperature and efficiency also occur at solar noon which are 93.4°C and 56.7%, respectively. Hot water temperature exceeds 90°C for 3 hours and is above 80°C for 7 hours per day. After 4:30 PM there is no useful energy gain (winter season). Daily energy gain, by 1 m^2 of the collector absorber, is 11.36 MJ/m^2.day which is equal to 3.16 kWh.

5.3 Performance and Output of the Absorption System

Very few studies can be traced in literature that give the performance of a solar absorption refrigeration system at more than its design point. A prominent feature available in *Cycle-Tempo* software is its potential to simulate the system when operated under off-design conditions. In this study the whole system was designed to provide its full cooling power at solar noon during the month of May (100kW peak cooling power). Like the situation of all solar driven systems, most of the time absorption refrigeration system will be working at off-design conditions.

5.3.1 System Analysis at Base Condition

Results of thermodynamic analysis for the system at the base condition are demonstrated in Table 4. For further comprehension of the system's irreversibility, the T-S diagram is presented in Figure 12.

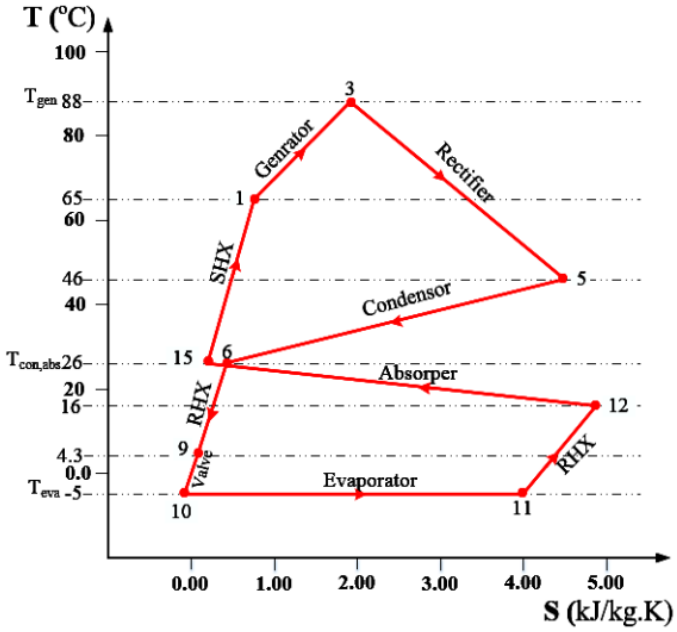

Fig. 12. Real NH_3/H_2O single effect absorption cycle on T – S diagram.

Table 4. Results of the system analysis at the base condition.

State No.	Mass flow (kg/s)	Pressure (bar)	Temp. (°C)	Enthalpy (kJ/kg)	NH_3 Mass Fraction	Medium	Exergy Ė (kW)	Exergy E (kJ/kg)	Entropy s (kJ/kg.K)
1	0.452	10.32	65	54.76	0.5000	NH_3-H_2O	17.42	38.56	0.7688
2	0.460	10.32	64.5	49.07	0.5000	NH_3-H_2O	17.46	37.97	0.7517
3	0.100	10.32	88.1	1492.71	0.9609	NH_3-H_2O	44.70	97.20	1.9242
4	0.360	10.32	88.1	169.33	0.3714	NH_3-H_2O	10.91	30.35	1.0806
5	0.115	10.32	46.2	1344.16	0.9980	NH_3-H_2O	37.33	324.49	4.5167
6	0.115	10.32	26	120.87	0.9980	NH_3-H_2O	36.48	317.15	0.4384
7	0.023	10.32	26	120.87	0.9980	NH_3-H_2O	7.30	317.15	0.4384
8	0.092	10.32	26	120.87	0.9980	NH_3-H_2O	29.19	317.15	0.4384
9	0.092	10.32	4.3	18.66	0.9980	NH_3-H_2O	25.51	320.66	0.0838
10	0.092	3.50	-5.28	-25.69	0.9980	NH_3-H_2O	29.78	323.65	-0.0750
11	0.092	3.50	-5.00	1061.73	0.9980	NH_3-H_2O	18.49	200.97	3.9837
12	0.092	3.50	16.01	1305.18	0.9980	NH_3-H_2O	16.27	176.77	4.8814
13	0.360	10.32	39	-56.11	0.3714	NH_3-H_2O	1.76	4.9	0.4098
14	0.360	3.50	39.1	-56.11	0.3714	NH_3-H_2O	1.49	4.14	0.4123
15	0.452	3.256	26	-126.18	0.5000	NH_3-H_2O	11.75	26.02	0.2040
16	0.452	10.84	26.7	-124.74	0.5000	NH_3-H_2O	12.17	26.96	0.2057
17	4.470	3	96.1	402.81	-	Water	1331.55	30.94	1.2626
18	4.470	3	86.1	360.76	-	Water	104.17	23.30	1.147

5.3.2 Cooling Production and CR

Figure 13 implies the solar absorption refrigeration system output during the months of May and December. As presented, during May (the summer season in Dongola) the system can run daily for 8 hours to produce 591.2 kWh cooling power. This power is equivalent to 24.6 kWh for 24 hours average. The cold production touches its peak (100 kW) at solar noon when hot water and T_{gen} are maximum. At this time the required flow rate of hot water from solar collectors to the generator is 4.47 kg/sec. For this flow rate, 224 collectors (which has 756m^2 total absorber surface area) are required to supply the absorption system with hot water. Before 8:30 AM the cold production is very low. Similarly, 3:30 PM onwards it decreases dramatically. In addition, the system requires high pumping power due to high circulation ratio as appears in Figure 14. So the system operation may become inefficient beyond this time limit.

In the month of December (winter time in Wadi-Halfa), the system can be operated for 7 hours to produce 490 kWh cooling power per day (20.4 kWh for 24 hours average). After 3:30 PM the output is in a short

supply. Peak cooling power is 92.2 kW which occurs at solar noon. During this month the system output cannot reach the designed value due to low solar irradiation. The daily cooling production drops by about 101.2 kWh per day during December as compared with that obtained during May.

Figure 14 revealed that for same time hours, the circulation ratio (CR) in May is lower than that of December. Its minimum value is 3.93 which happens in May at solar noon (11:30 – 12:30). However for times of low solar irradiation, the CR can reach high values so that the system operation becomes inefficient.

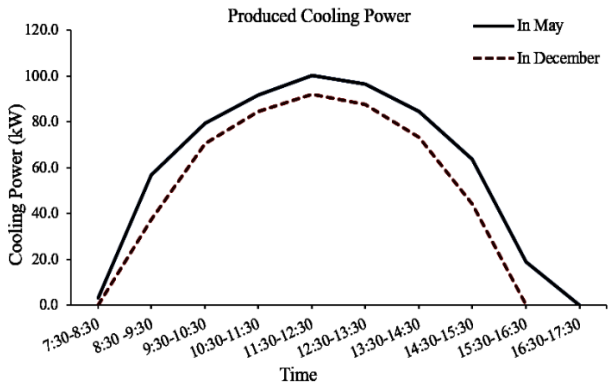

Fig. 13. Daily cooling production in the months of May and December.

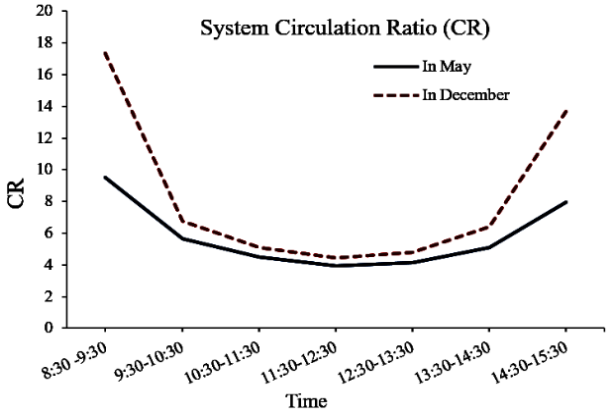

Fig. 14. System's circulation ratio in the months of May and December.

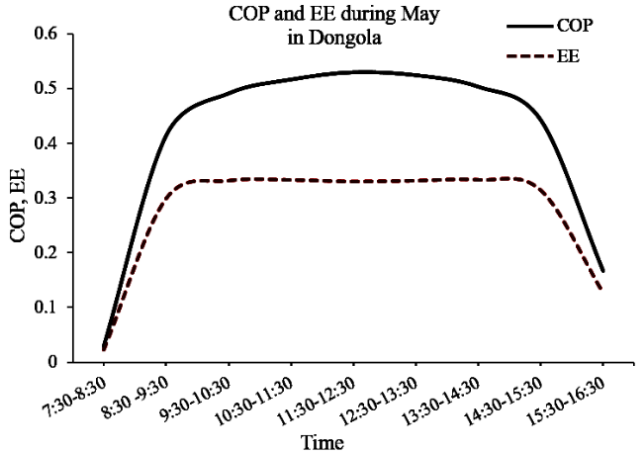

Fig. 15. The daily system's performance during the month of May.

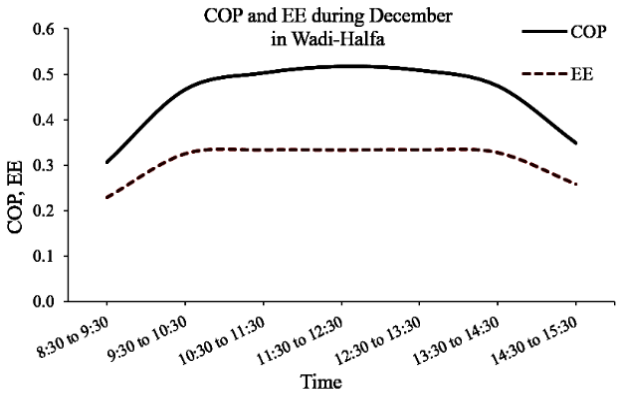

Fig. 16. The daily system's performance during the month of December.

5.3.3 System's Energetic Performance

Figure 15 expresses daily coefficient of performance (COP) for the system during the month of May in Dongola. In this month the system output meets its designed value (100 kW). Consequently COP reaches its maximum (0.5292). It takes place at solar noon when hot water temperature and collectors efficiency are at their maximum values. During this month the daily average value of COP is 0.4481 (for 8 working hours). Nevertheless, it is above 0.41 for 7 hours per day. During these 7 hours T_{gen} remains over 80^{o}C for 5 hours which let the system working near its base design condition for longer time than other months. During this month the daily average system efficiency is about 10.4% (daily cold production divided by daily solar energy incident on solar collectors).

In December as portrayed by Figure 16, low amount of solar radiation incident on the solar collectors (winter season in Wadi-Halfa). This leads to a lower hot water temperature from collectors array to absorption system, followed by lower T_{gen} which directly affects the system output and hence decreases the COP. Daily average of COP is 0.446 (for 7 working hours). The maximum value of COP is 0.5171 which occurs at solar noon when T_{gen} is 85.5^{o}C. During this month the daily average system efficiency is about 9.2% (on the base of total collector absorber surface area). By merging these results it can be summarized that the daily maximum COP ranges from 0.5292 to 0.5171and the daily average comes within the range of 0.4481 – 0.4460.

5.3.4 System's Energetic Performance

Daily exergy efficiency for the system during the month of May in Dongola is displayed in Figure 15. Compared with the coefficient of performance, the EE displays a slightly different tendency. It is at low values in starting hours when the system starts working with low T_{gen}. As the generator temperature increases, the EE increases due to more exergy gained by evaporator. This situation continues till EE reaches its maximum value (0.3332) at T_{gen} of 83°C. This appears at the hour 10:30 – 11:30 before solar noon. Thereafter it marginally decreases for two hours when T_{gen} is above 85°C and resume its maximum for the hour 13:30 – 14:30 when the temperature of generator returns to be 83°C. Decrease of EE at higher T_{gen} can be caused by the increase of exergy losses at higher solution temperature in generator, absorber and SHX. These results are consistent with previous in [17], [34]. Later on, the EE decreases tremendously with the decrease of cooling production. Its average value is 0.2999 for 8 working hours per day.

The exergy efficiency for working hours during December at Wadi-Halfa is plotted in Figure 16. During this period of year, T_{gen} remains at relatively low values (below 85.5°C). Therefore value of EE stays near maximum for 5 hours out of 7 per day with daily average value of 0.3054. So it can be determined that the maximum achieved exergy efficiency during the year marginally ranges from 0.3335 to 0.3332. Similarly, the daily average is from 0.3054 to 0.2999.

Figures 17 and 18 compare the hourly produced cooling power with energy gained by collector field and energy irradiated on the collector field which is termed as available solar energy.

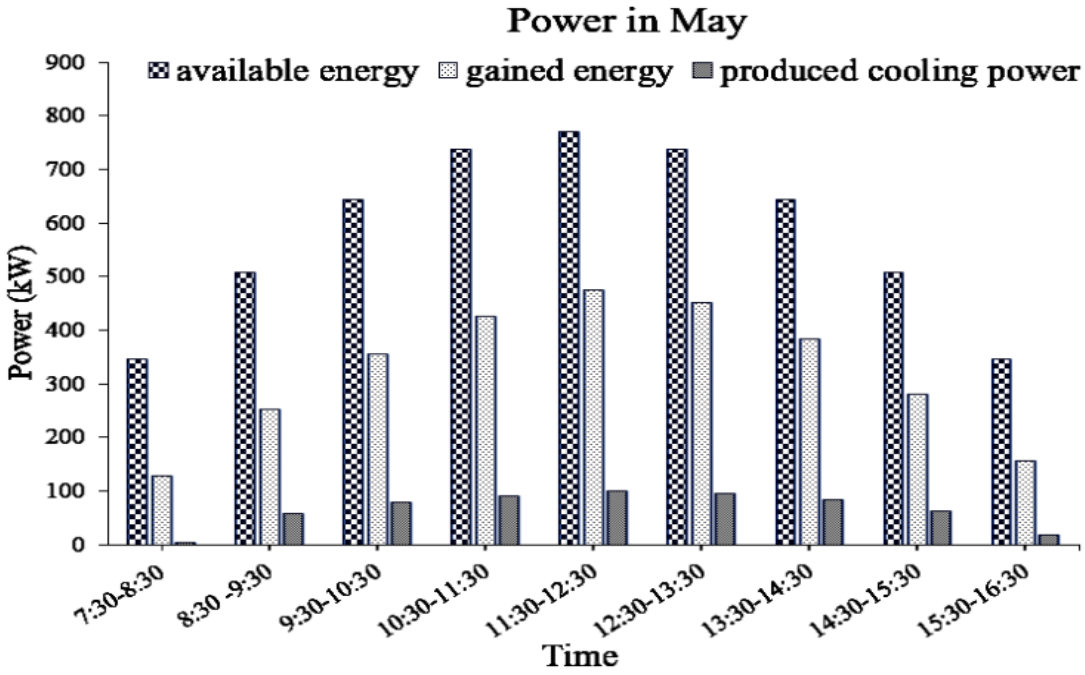

Fig. 17. Available, gained and cooling power in the month of May.

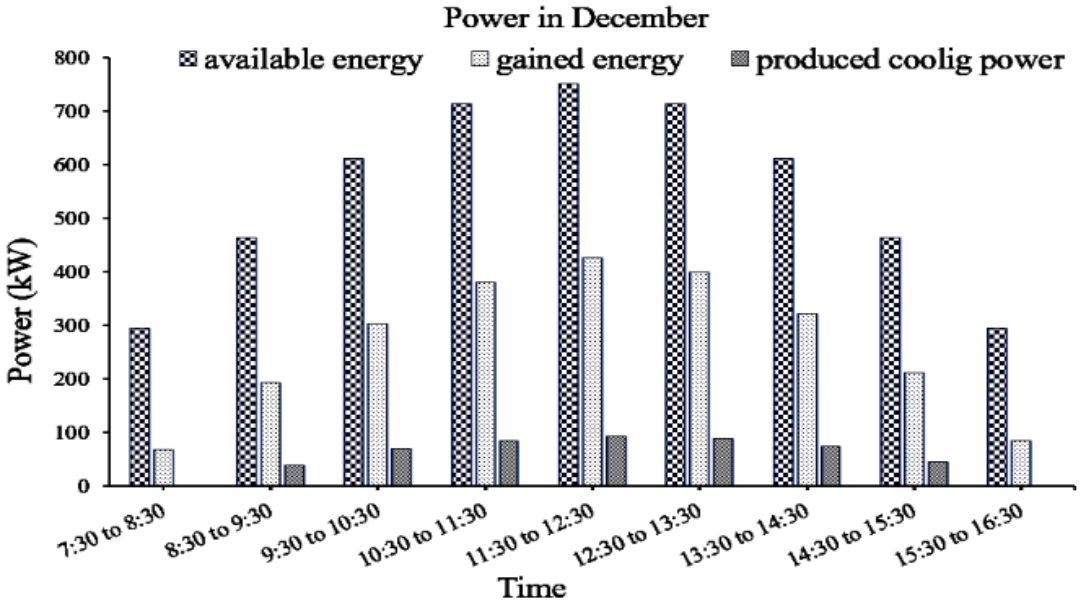

Fig. 18. Available, gained and cooling power in the month of December.

6. CONCLUSION AND RECOMMENDATIONS

The region of Northern Sudan fetches ample source of solar energy which can be developed to supplement the current stock of traditional resources. In addition, the solar radiation in this region has an expedient and distinctive characteristic; that is the differences in global solar radiation are relatively small throughout the year. This feature plays a pivotal role in solar energy utilization.

In this study, the performance and output of solar driven NH_3/H_2O absorption refrigeration system have been investigated under climate of the region of Northern Sudan. The system is operated by high performance flat-plate solar collector and designed to give 100 kW peak cooling power. Simulation has been performed by using the minimum and maximum values of available solar energy in the region. The results interpreted that the system can deliver its maximum power during the month of May. In this month, the system can work effectively for 8 hours daily to produce 591.2 kWh cooling power with daily averages of COP and EE as 0.4481 and 0.2999, respectively.

The minimum output is received in December during winter season in the region. Daily output is 490 kWh produced in 7 hours with daily averages of COP and EE as 0.446 and 0.3335, respectively. However this reduction in output seems to be compensated by the fact that need for cooling is significantly decreased in winter time.

The study result also demonstrates that the well-designed flat-plate solar collector is capable to drive absorption refrigeration system in the region of Northern Sudan throughout the year with acceptable performance. Use of this collector type can successfully contribute towards the reduction of system's initial cost in the study area and other places that possess similar quantities of high solar irradiation

NOMENCLATURE

COP	Coefficient of performance
EE	Exergy efficiency
FPC	Flat-plate collector
SHX	Solution heat exchanger
RHX	Refrigerant heat exchanger
ARS	Absorption refrigeration system
A	Area (m^2)
S	Absorbed solar radiation (Wm^{-2})
P	Pressure (kPa)
$\dot{Q}$	Heat energy (kW)
$\dot{W}$	Pump power (kW)
CR	Circulation ratio
$\dot{m}$	Mass flow rate ($kg\ s^{-1}$)
c_p	Specific heat ($kJ\ kg^{-1}K^{-1}$)
U_L	Overall heat loss coefficient ($Wm^{-2}K^{-1}$)
F_R	Collector heat removal factor
G_T	incident solar radiation (Wm^{-2})
h	Specific enthalpy ($kJ\ kg^{-1}$)
s	Specific entropy ($kJ\ kg^{-1}K^{-1}$)
$\dot{E}$	Exergy rate (kW)
E	Specific exergy (kJ kg -1)
T	Temperature (°C)

Subscripts

gen	Generator
con	Condenser
eva	Evaporator
abs	Absorber
ss	Strong solution
r	refrigerant
pump	Solution pump
pm	Mean absorber plate
i	Inlet
a	Ambient
o	Reference state
p	Collector aperture
c	Collector
d	Diffuse radiation
u	Useful gain

Greek symbols

η	Efficiency
α	Absorptance of collector plate
τ	Transmittance of collector cover
ρ	Reflectance of cover system
ε	Absorber emittance
Δ	Difference in any quantity

REFERENCES

[1] Fong K., Chow T.T., Lee C.K., Lin Z. and Chan L., 2010. Comparative study of different solar cooling systems for buildings in subtropical city. *Solar Energy* 84(2): 227-244.

[2] Heryadi M.D. and D. Hartono. 2016. Energy efficiency, utilization of renewable energies, and carbon dioxide emission: case study of G20 countries. *International Energy Journal* 16(4): 143-152.

[3] Said S., Spindler K., El-Shaarawi M., Siddiqui M., Schmid F., Bierling B. and Khan M. 2016., 2016. Design, construction and operation of a solar powered ammonia–water absorption refrigeration system in Saudi Arabia. *International Journal of Refrigeration* 62: 222-231.

[4] Rostamzadeh H., Ghaebi H. and Behnam F., 2017. Energetic and exergetic analyses of modified combined power and ejector refrigeration cycles. *Thermal Science and Engineering Progress* 2: 119-139.

[5] Balaras C., Grossman G., Henning H., Ferreira C., Podesser E., Wang L. and Wiemken E., 2007. Solar air conditioning in Europe—an overview. *Renewable and Sustainable Energy Reviews* 11(2): 299-314.

[6] Mohammed O.W., 2012. Study and Analysis of a Solar Absorption Refrigeration System in Northern Sudan. *MS Thesis.* Nile Valley University, Atbara, Sudan.

[7] Peel M.C., Finlayson B.L. and McMahon T.A., 2007. Updated world map of the Köppen-Geiger

climate classification. *Hydrology and Earth System Sciences Discussions* 4(2): 439-473.

[8] Mohammed O.W. and G. Yanling, 2016. Estimation of diffuse solar radiation in the region of Northern Sudan. *International Energy Journal*16(4): 163-172.

[9] Omer A.M.,1997. Compilation and evaluation of solar and wind energy resources in Sudan. *Renewable Energy* 12(1): 39-69.

[10] Diabate L., Blanc P. and Wald L., 2004. Solar radiation climate in Africa. *Solar Energy* 76(6): 733-744.

[11] Kalogirou S.A., 2013. *Solar energy engineering: processes and systems*, 1st edition. Burlington, USA: Academic Press.

[12] Duffie J.A. and W.A. Beckman. 2013. *Solar Engineering of Thermal Processes*, 4thedition. Hoboken, New Jersey: John Wiley & Sons.

[13] Zhang K., Hao L., Du M., Mi J., Wang J.N. and Meng J.P., 2017. A review on thermal stability and high temperature induced ageing mechanisms of solar absorber coatings. *Renewable and Sustainable Energy Reviews* 67: 1282-1299.

[14] Li Q., Zheng C., Shirazi A., Mousa O., Moscia F., Scott J. and Taylor R., 2017. Design and analysis of a medium-temperature, concentrated solar thermal collector for air-conditioning applications. *Applied Energy* 190: 1159-1173.

[15] Sarbu I. and C. Sebarchievici. 2015. General review of solar-powered closed sorption refrigeration systems. *Energy Conversion and Management* 105: 403-422.

[16] Siddiqui M. and S. Said. 2015. A review of solar powered absorption systems. *Renewable and Sustainable Energy Reviews* 42: 93-115.

[17] Aman J., Ting D.K. and Henshaw P., 2014. Residential solar air conditioning: Energy and exergy analyses of an ammonia–water absorption cooling system. *Applied Thermal Engineering* 62(2): 424-432.

[18] Hepbasli A., 2008. A key review on exergetic analysis and assessment of renewable energy resources for a sustainable future.*Renewable and Sustainable Energy Reviews* 12(3): 593-661.

[19] Rostamzadeh H., Ebadollahi M., Ghaebi H., Amidpour M. and Kheiri R., 2017. Energy and exergy analysis of novel combined cooling and power (CCP) cycles. *Applied Thermal Engineering* 124: 152-169.

[20] Habibzadeh A., Rashidi M. and Galanis N., 2013. Analysis of a combined power and ejector-refrigeration cycle using low temperature heat. *Energy Conversion and Management* 65: 381-391.

[21] Alvares S. and C. Trepp. 1987. Simulation of a solar driven aqua-ammonia absorption refrigeration system Part 1: mathematical description and system optimization. *International Journal of Refrigeration* 10(1): 40-48.

[22] Sözen A., Altıparmak D. and Usta H., 2002. Development and testing of a prototype of absorption heat pump system operated by solar energy. *Applied Thermal Engineering* 22(16): 1847-1859.

[23] Sloetjes W. Haverhals J., Kerkdijk K., Ahmed I., Saber H., Shaa-Eldin S., Porsius R. Stolk A., El Karib A. and Yousif K., 1988. Operational results of the 13 kW/50 m^3 solar-driven cold store in Khartoum, the Sudan. *Solar Energy* 41(4): 341-347.

[24] Zaki M., 2010. Design and Construction of a continuous solar absorption refrigeration Unit. Ph.D Thesis. University of Khartoum, Khartoum, Sudan.

[25] Kim D. and C.I. Ferreira. 2008. Solar refrigeration options–a state-of-the-art review. *International Journal of Refrigeration* 31(1): 3-15.

[26] Colonna P. and S. Gabrielli. 2003. Industrial trigeneration using ammonia–water absorption refrigeration systems (AAR). *Applied Thermal Engineering* 23(4): 381-396.

[27] Sözen A., 2001. Effect of heat exchangers on performance of absorption refrigeration systems. *Energy Conversion and Management* 42(14): 1699-1716.

[28] Singh O.K. and S. Kaushik. 2013. Thermoeconomic evaluation and optimization of a Brayton–Rankine–Kalina combined triple power cycle. *Energy Conversion and Management* 71: 32-42.

[29] Bejan A. and G. Tsatsaronis. 1996. *Thermal Design and Optimization.* Hoboken, New Jersey: John Wiley & Sons.

[30] Woudstra N. and T. Van der Stelt. 2002. Cycle-Tempo: a program for the thermodynamic analysis and optimization of systems for the production of electricity, heat and refrigeration. *Energy Technology Section.* Delft University of Technology: Delft, The Netherlands.

[31] Ziegler B. and C. Trepp. 1984. Equation of state for ammonia-water mixtures. *International Journal of Refrigeration* 7(2): 101-106.

[32] Koo J.M., 1999. Development of a flat-plate solar collector design program. *MS Thesis.* University of Wisconsin-Madison, USA.

[33] Best R., Islas J. and Martinez M., 1993.Exergy efficiency of an ammonia-water absorption system for ice production. *Applied Energy* 45(3): 241-256.

[34] Táboas F., Bourouis M. and Vallès M., 2014. Analysis of ammonia/water and ammonia/salt mixture absorption cycles for refrigeration purposes in fishing ships. *Applied Thermal Engineering* 66(1): 603-611.